

Periodic Output Feedback for Spatial Control of AHWR: A Three-Time-Scale Approach

R. K. Munje, B. M. Patre, and A. P. Tiwari

Abstract—This paper presents a novel technique of designing Periodic Output Feedback (POF) based controller for three-time-scale systems. This design method is investigated for spatial control of Advanced Heavy Water Reactor (AHWR). The numerically ill-conditioned system of AHWR is first decomposed into three subsystems, namely, slow, fast 1 and fast 2 by direct block-diagonalization and then a composite controller is designed which provides an output injection gain. This output injection gain has been used to compute POF gain, which is then applied to the vectorized non-linear model of AHWR to achieve spatial control. This controller is tested via simulations carried out under different transient conditions and the results of simulation are presented.

Index Terms—Advanced heavy water reactor, periodic output feedback, spatial control, three-time-scale system.

I. INTRODUCTION

SINGULAR perturbations and time-scale methods are popular methods for model order reduction and controller design [1], [2]. These methods work by decoupling the fast and slow varying phenomena. A number of state feedback based approaches have been developed over the period of time to tackle the ill-conditioning generally observed in case of higher order systems [3]–[6]. The practical implementation of such a state feedback based controller, however, demands a state observer of large order. Hence, it is desirable to go for an output feedback design. The static output feedback is one of the most investigated problems in the control theory and applications [7]. However, in this approach the stability of the closed loop system is not guaranteed. In [8], it is shown that, if a system is controllable and observable, then for almost all output sampling rates any self-conjugate pole configuration can be assigned to the discrete-time closed loop system by piecewise constant output feedback, provided the number of gain changes is not less than the system's controllability index. Multirate Output Feedback (MROF) is the concept of sampling the system input and system output at different rates. Periodic

Output Feedback (POF) is the kind of MROF in which system output is sampled at slower rate than the input [9]. Formulation of POF for two-time-scale systems is reported in [10]–[13]. In [12], the POF controller for two-time-scale system is obtained by combining the solutions of slow and fast subsystem problems, obtained separately. Thus, ill-conditioning is completely avoided and two lower order problems are solved instead of one higher order problem. Design of POF controller for spatial control of nuclear reactors can be found in [14], [15].

In this paper, the idea of [12] is extended for three-time-scale systems and it is examined for spatial stabilization of Advanced Heavy Water Reactor (AHWR). Rest of the paper is organized in the following sequence. In Section II AHWR system is discussed. Section III presents proposed control strategy. The application of control strategy to AHWR and transient simulations are demonstrated in Section IV, followed by the conclusion in Section V and the references.

II. OVERVIEW OF AHWR

AHWR is a 920 MW(thermal), vertical pressure tube type reactor, moderated by heavy water, cooled by boiling light water and fueled with (Th – ²³³U)O₂ and (Th-Pu)O₂ pins [16]. The reactivity control devices in AHWR consist of eight absorber rods (ARs), eight shim rods (SRs) and eight regulating rods (RRs). The AHWR core has physical dimension much greater than the neutron migration length causing xenon induced spatial oscillations in power [17]. This necessitates regulation of total as well as spatial power over time. The AHWR model developed in [18] and [19] has been used here for the study carried out in this paper. The AHWR core is considered to be divided in 17 relatively large nodes as shown in Fig. 1. The following non-linear equations constitute the mathematical model of AHWR [18]–[20]:

$$\frac{dP_i}{dt} = (\rho_i - \alpha_{ii} - \beta) \frac{P_i}{\ell} + \sum_{j=1}^{17} \alpha_{ji} \frac{P_j}{\ell} + \lambda C_i \quad (1)$$

$$\frac{dC_i}{dt} = \frac{\beta}{\ell} P_i - \lambda C_i \quad (2)$$

$$\frac{dI_i}{dt} = \gamma_I \Sigma_{fi} P_i - \lambda_I I_i \quad (3)$$

$$\frac{dX_i}{dt} = \gamma_X \Sigma_{fi} P_i + \lambda_I I_i - (\lambda_X + \bar{\sigma}_{Xi} P_i) X_i \quad (4)$$

$$\frac{dH_k}{dt} = \kappa v_k \quad (5)$$

$$e_{vx_i} \frac{dx_i}{dt} = P_i - q_{d_i}(h_w - h_d) - q_{d_i} x_i h_c \quad (6)$$

$$e_{xh} \frac{dh_d}{dt} = q_f(\hat{k}_2 h_f - \hat{k}_1) - q_d(\hat{k}_2 h_d - \hat{k}_1) \quad (7)$$

Manuscript received February 19, 2014; revised May 07, 2014; accepted May 26, 2014. Date of publication July 25, 2014; date of current version August 14, 2014.

R. K. Munje is with K.K. Wagh Institute of Engineering Education and Research, Nashik-422003, India, and also with the S.G.G.S. Institute of Engineering and Technology, Vishnupuri, Nanded-431606, India (e-mail: ravimunjje@yahoo.co.in).

B. M. Patre is with the Department of Instrumentation Engineering, S.G.G.S. Institute of Engineering and Technology, Vishnupuri, Nanded-431606, India (e-mail: bmpatre@ieee.org).

A. P. Tiwari is with the Reactor Control Division, Bhabha Atomic Research Centre, Trombay, Mumbai-400085, India (e-mail: aptiwari@barc.gov.in).

Color versions of one or more of the figures in this paper are available online at <http://ieeexplore.ieee.org>.

Digital Object Identifier 10.1109/TNS.2014.2327691

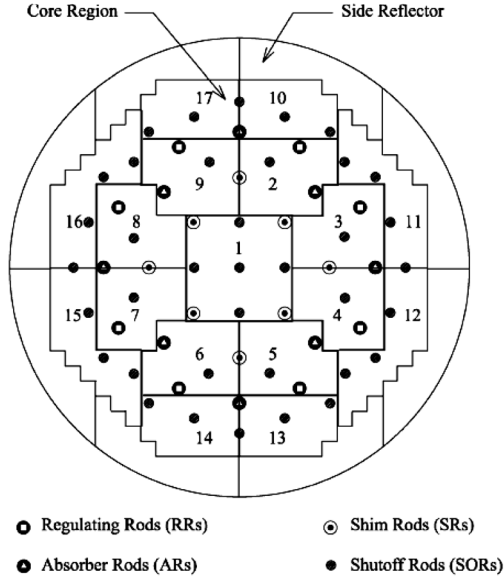


Fig. 1. 17 nodes AHWR scheme.

where $k = 2, 4, 6, 8$ and $i = 1, 2, \dots, 17$. P, C, I, X and H are nodal powers, effective one group delayed neutron precursor, iodine and xenon concentrations and regulating rod positions respectively. x_i and h_d denote exit quality of i th node and down-comer enthalpy respectively. α_{ji} and α_{ii} denote the coupling coefficients between j th and i th nodes and self coupling coefficients of i th node respectively. $\bar{\sigma}_{Xi} = \sigma_{Xfi}/E_{eff}\Sigma_{fi}V_i$ and v_k is control signal applied to the RR drive and κ is a constant having value 0.56. Other notations and symbols have their usual meanings.

Values of $e_{v_{xi}}$ and e_{x_h} alongwith neutronic parameters, nodal volumes and cross-sections, nodal powers, coolant flow rates under full power operation and coupling coefficients are given in [21]. The reactivity term ρ_i in (1) is expressed as $\rho_i = \rho_{i_u} + \rho_{i_X} + \rho_{i_\alpha}$, where ρ_{i_u} , ρ_{i_X} and ρ_{i_α} are the reactivity feedbacks due to the control rods, xenon and coolant void fraction respectively, given by

$$\rho_{i_u} = \begin{cases} (-10.234H_i + 676.203) \times 10^{-6}, & \text{if } i = 2, 4, 6, 8. \\ 0 & \text{elsewhere,} \end{cases}$$

$$\rho_{i_X} = -\frac{\bar{\sigma}_{Xi}X_i}{\Sigma_{ai}},$$

$$\rho_{i_\alpha} = -5 \times 10^{-3}(9.2832x_i^5 - 27.7192x_i^4 + 31.7643x_i^3 - 17.7389x_i^2 + 5.2308x_i + 0.0792).$$

Equations (1)-(7) are linearized around steady state operating conditions ($H_{k0}, X_{i0}, I_{i0}, h_{d0}, C_{i0}, x_{i0}, P_{i0}$) and represented in standard state space form. For this, define the state vector as

$$z = [z_H^T \quad z_X^T \quad z_I^T \quad \delta h_d \quad z_C^T \quad z_x^T \quad z_P^T]^T \quad (8)$$

where $z_H = [\delta H_2 \quad \delta H_4 \quad \delta H_6 \quad \delta H_8]^T$ and the rest $z_\xi = [(\delta \xi_1/\xi_{10}) \quad \dots \quad (\delta \xi_{17}/\xi_{170})]^T$, $\xi = X, I, C, x, P$, in which δ denotes the deviation from respective steady state value of the variable. Likewise, define the input vector

as $u = [\delta v_2 \quad \delta v_4 \quad \delta v_6 \quad \delta v_8]^T$ and output vector as $y = [y_g \quad y_1 \quad \dots \quad y_{17}]^T$ where

$$y_g = \sum_{i=1}^{17} \frac{\delta P_i}{\sum_{j=1}^{17} P_{j0}}$$

and $y_i = \frac{\delta P_i}{P_{i0}}$ correspond to normalized total reactor power and nodal powers respectively. Then, the system given by (1)-(7) can be expressed in standard linear state space form as

$$\dot{z} = Az + Bu + B_f \delta q_f \quad (9)$$

$$y = Mz \quad (10)$$

where δq_f is deviation in feed water flow rate. Matrices A, B, B_f and M are given in [21]. The six eigenvalues of A with positive real parts besides the four eigenvalues at the origin indicate instability. Hence, it is necessary to design an effective spatial controller for AHWR.

Spatial oscillations in neutron flux distribution resulting from xenon reactivity feedback are a matter of concern in large nuclear reactors, like AHWR. If these spatial oscillations are not controlled, power density and rate of change of power at some locations in the reactor core may exceed limits of fuel failure [17]. Spatial control of AHWR, that means to suppress xenon oscillations from growing, has been attempted in [21], [22] using static output feedback. But, static output feedback does not guarantee stability of closed loop system [7]. Hence, as an extension to this, Shimjith *et al.* have applied state feedback based approach [3] to AHWR. However, this requires a state observer of large order for practical implementation, which increases implementation cost and reduces the reliability of control system. To overcome this, MROF based Fast Output Sampling (FOS) control technique is investigated in [23]. The control techniques presented in [3] and [23] are based on system decomposition, in which the numerically ill-conditioned system of AHWR is decomposed into three subsystems, namely, slow, fast 1 and fast 2. The control gains for original system are obtained by combining the solutions of the three subsystem problems, obtained separately. In FOS, control signal is generated as a linear combination of a number of output samples collected in one sampling interval. In this, input sampling time is larger compared to output sampling time. For example in [23], sampling time for spatial control component of input is taken as 60 s. A similar kind of approach for two-time-scale system is suggested in [24] for the AHWR, where sampling time is taken as 54 s. However, for practical reactor control to work with larger sampling time is not desirable, because in small time, reactor can undergo a considerable change. Recently, a single-input fuzzy logic controller has been proposed for spatial control of AHWR [25]. Munje *et al.* have explored the application of robust Sliding Mode Control (SMC) technique to AHWR [26]. Though it is shown that, better results are obtained, compared to other control techniques, it requires all the states for feedback.

In this paper, periodic output feedback based technique is used for spatial control purpose. The mathematical model of the AHWR is of very high order and numerically ill-conditioned, making the control problem difficult to solve. Fortunately however, the three-time-scale property exhibited by the

model can be exploited to simplify the problem. Hence, the higher order system of AHWR is decomposed into three subsystems by three-time-scale decomposition presented in [5]. These smaller order problems are then separately solved and the results thus obtained for subsystems are combined to obtain the composite output injection gain for the original system, from which POF controller is derived. Using this POF controller, nonlinear system of AHWR is simulated and results are generated for different transient conditions.

III. PROPOSED CONTROL APPROACH

A. Overview of Periodic Output Feedback

Consider a linear time-invariant controllable and observable continuous-time model

$$\dot{z}(t) = Az(t) + Bu(t) \quad (11)$$

$$y(t) = Mz(t) \quad (12)$$

where $z \in \mathfrak{R}^n$, $u \in \mathfrak{R}^m$, $y \in \mathfrak{R}^p$ and A , B and M are constant matrices of appropriate dimensions. System (11)-(12) when sampled at the rate of $1/\tau$ gives discrete-time model as

$$z((k+1)\tau) = \Phi_\tau z(k\tau) + \Gamma_\tau u(k\tau) \quad (13)$$

$$y(k\tau) = Mz(k\tau) \quad (14)$$

where $\Phi_\tau = e^{A\tau}$ and $\Gamma_\tau = \int_0^\tau e^{As}Bds$. Also, let

$$z(k+1) = \Phi_\Delta z(k) + \Gamma_\Delta u(k) \quad (15)$$

be the discrete-time system corresponding to the system (11) sampled at the rate $1/\Delta$, where $\Delta = \tau/N$, where $N \geq \mu$, the controllability index [27] of (Φ_τ, Γ_τ) . The output is measured at the time instants $t = k\tau$, $k = 0, 1, \dots$ using a sample and hold system. The output sampling interval τ is divided into N subintervals of length Δ and the input is generated according the following control law

$$u(t) = K_l y(k\tau), \quad k\tau + l\Delta \leq t \leq k\tau + (l+1)\Delta, \\ K_{l+N} = K_l, \quad l = 0, 1, 2, \dots, (N-1). \quad (16)$$

A sequence of N gain matrices $\{K_0, K_1, \dots, K_{N-1}\}$ when substituted in (16) generates a time-varying, piecewise constant output feedback gain $K(t)$ for $0 \leq t \leq \tau$. Define,

$$\mathbf{K} = [K_0^T K_1^T \dots K_{N-1}^T]^T \quad (17)$$

and

$$\mathbf{u}(k\tau) = \mathbf{K}y(k\tau) = \begin{bmatrix} u(k\tau) \\ u(k\tau + \Delta) \\ \vdots \\ u(k\tau + \tau - \Delta) \end{bmatrix}, \quad (18)$$

then a state space representation for the system (13) is obtained as

$$z((k+1)\tau) = \Phi_\Delta^N z(k\tau) + \mathbf{\Gamma} \mathbf{u}(k\tau) \quad (19)$$

where

$$\mathbf{\Gamma} = [\Phi_\Delta^{N-1} \Gamma_\Delta \Phi_\Delta^{N-2} \Gamma_\Delta \dots \Gamma_\Delta]. \quad (20)$$

From (14), (18) and (19), the closed loop system becomes

$$z((k+1)\tau) = (\Phi_\Delta^N + \mathbf{\Gamma} \mathbf{K} M) z(k\tau). \quad (21)$$

Let G be the stabilizing output injection gain for (13)-(14) i.e.

$$\varphi(\Phi_\tau + GM) < 1. \quad (22)$$

where $\varphi(\cdot)$ denotes the spectral radius. It is evident from (21) and (22) that G is realizable through \mathbf{K} , if and only if

$$\mathbf{\Gamma} \mathbf{K} = G. \quad (23)$$

As (11)-(12) is controllable and observable, the system (13)-(14) is also generically controllable and observable. So the existence of \mathbf{K} is guaranteed if number of gain changes is larger than or equal to the controllability index i.e. if $N \geq \mu$.

B. POF Based Controller for Three-Time-Scale System

Consider that linear time-invariant discrete-time system given by (13), possesses three-time-scale property so that it can be represented as

$$\begin{bmatrix} z_{1k+1} \\ z_{2k+1} \\ z_{3k+1} \end{bmatrix} = \begin{bmatrix} \Phi_{11} & \Phi_{12} & \Phi_{13} \\ \Phi_{21} & \Phi_{22} & \Phi_{23} \\ \Phi_{31} & \Phi_{32} & \Phi_{33} \end{bmatrix} \begin{bmatrix} z_{1k} \\ z_{2k} \\ z_{3k} \end{bmatrix} + \begin{bmatrix} \Gamma_1 \\ \Gamma_2 \\ \Gamma_3 \end{bmatrix} u_k \quad (24)$$

$$y_k = [M_1 \quad M_2 \quad M_3] [z_{1k}^T \quad z_{2k}^T \quad z_{3k}^T]^T \quad (25)$$

where $z_{1k} \in \mathfrak{R}^{n_1}$ denotes the slowly varying states, $z_{2k} \in \mathfrak{R}^{n_2}$ denotes the fast varying states and $z_{3k} \in \mathfrak{R}^{n_3}$ denotes the states which vary even faster ($n_1 + n_2 + n_3 = n$) and the matrices Φ_{ij} , Γ_i and M_i are of appropriate dimensions. Let $\varphi(\Phi_\tau)$ be the eigenvalues of matrix Φ_τ arranged in decreasing order of absolute values as

$$\varphi(\Phi_\tau) = \{\varphi_1, \dots, \varphi_{n_1}, \varphi_{n_1+1}, \dots, \varphi_{n_1+n_2}, \varphi_{n_1+n_2+1}, \dots, \varphi_n\},$$

where

$$|\varphi_1| > \dots > |\varphi_{n_1}| \gg |\varphi_{n_1+1}| > \dots \\ > |\varphi_{n_1+n_2}| \gg |\varphi_{n_1+n_2+1}| > \dots > |\varphi_n| \geq 0.$$

Thus the system (24) possesses three distinct groups of eigenvalues such that n_1 eigenvalues are close to the unit circle and n_2 and n_3 eigenvalues are respectively far and farther from the unit circle towards the origin. Alternatively, the system (24) has n_1 “slow” modes, n_2 “fast” modes and n_3 “fastest” modes. System (24)-(25) can be decoupled into three subsystems [5], [23] named slow, fast 1 and fast 2 respectively, and represented in block-diagonal form as

$$\begin{bmatrix} z_{s_{k+1}} \\ z_{f1_{k+1}} \\ z_{f2_{k+1}} \end{bmatrix} = \begin{bmatrix} \Phi_{\tau s} & 0 & 0 \\ 0 & \Phi_{\tau f1} & 0 \\ 0 & 0 & \Phi_{\tau f2} \end{bmatrix} \begin{bmatrix} z_{s_k} \\ z_{f1_k} \\ z_{f2_k} \end{bmatrix} + \begin{bmatrix} \Gamma_{\tau s} \\ \Gamma_{\tau f1} \\ \Gamma_{\tau f2} \end{bmatrix} u_k \quad (26)$$

$$y_k = [M_s \quad M_{f1} \quad M_{f2}] [z_{s_k}^T \quad z_{f1_k}^T \quad z_{f2_k}^T]^T \quad (27)$$

where $z_{s_k} \in \mathfrak{R}^{n_1}$, $z_{f1_k} \in \mathfrak{R}^{n_2}$ and $z_{f2_k} \in \mathfrak{R}^{n_3}$ denote respectively slow, fast 1 and fast 2 states such that $n_1 + n_2 + n_3 = n$. States of systems (24) and (26) are related as

$$z_{d_k} = T z_k \quad (28)$$

where $z_k = [z_{1_k}^T z_{2_k}^T z_{3_k}^T]^T$, $z_{d_k} = [z_{s_k}^T z_{f1_k}^T z_{f2_k}^T]^T$ and transformation matrix $T \in \mathfrak{R}^{n \times n}$ [23]. System (24)-(25) is decoupled into three subsystems in (26)-(27), namely, the “slow” subsystem $(\Phi_{\tau s}, \Gamma_{\tau s}, M_s)$, the “fast 1” subsystem $(\Phi_{\tau f1}, \Gamma_{\tau f1}, M_{f1})$ and the “fast 2” subsystem $(\Phi_{\tau f2}, \Gamma_{\tau f2}, M_{f2})$, of orders n_1 , n_2 and n_3 respectively. In the similar manner, the discrete-time system equivalent of (15) for the sampling interval Δ can also be decoupled as

$$z_{d_{k+1}} = \begin{bmatrix} \Phi_{\Delta s} & 0 & 0 \\ 0 & \Phi_{\Delta f1} & 0 \\ 0 & 0 & \Phi_{\Delta f2} \end{bmatrix} z_{d_k} + \begin{bmatrix} \Gamma_{\Delta s} \\ \Gamma_{\Delta f1} \\ \Gamma_{\Delta f2} \end{bmatrix} u_k. \quad (29)$$

Design of a stabilizing output injection gain for three-time-scale system (26) is discussed in the Appendix. It is given by

$$G^T = [G_s^T \ 0 \ 0] + [0 \ G_{f1}^T \ 0] T_{d1} + [0 \ 0 \ G_{f2}^T] T_{d2} T_{d1} \\ = [G_1^T \ G_2^T \ G_3^T] \quad (30)$$

where G_s^T , G_{f1}^T and G_{f2}^T are the stabilizing output injection gains for slow, fast 1 and fast 2 subsystems respectively, and T_{d1} and T_{d2} are transformation matrices. Now, the following form of Γ in (20) for the system (26) is assumed

$$\Gamma = \begin{bmatrix} \Gamma_{s1} & \Gamma_{s2} & \Gamma_{s3} \\ \Gamma_{f11} & \Gamma_{f12} & \Gamma_{f13} \\ \Gamma_{f21} & \Gamma_{f22} & \Gamma_{f23} \end{bmatrix} \quad (31)$$

where submatrices $\Gamma_{s1} \in \mathfrak{R}^{(n_1 \times (n - \mu_{f2} - \mu_{f1}))m}$, $\Gamma_{s2} \in \mathfrak{R}^{n_1 \times \mu_{f1}m}$, $\Gamma_{s3} \in \mathfrak{R}^{n_1 \times \mu_{f2}m}$, $\Gamma_{f11} \in \mathfrak{R}^{(n_2 \times (n - \mu_{f2} - \mu_{f1}))m}$, $\Gamma_{f12} \in \mathfrak{R}^{n_2 \times \mu_{f1}m}$, $\Gamma_{f13} \in \mathfrak{R}^{n_2 \times \mu_{f2}m}$, $\Gamma_{f21} \in \mathfrak{R}^{n_3 \times (n - \mu_{f2} - \mu_{f1}))m}$, $\Gamma_{f22} \in \mathfrak{R}^{n_3 \times \mu_{f1}m}$ and $\Gamma_{f23} \in \mathfrak{R}^{n_3 \times \mu_{f2}m}$ are respectively given by

$$\Gamma_{s1} = [\Phi_{\Delta s}^{N-1} \Gamma_{\Delta s} \cdots \Phi_{\Delta s}^{N-\mu_s} \Gamma_{\Delta s}] \quad (32)$$

$$\Gamma_{s2} = [\Phi_{\Delta s}^{N-\mu_s-1} \Gamma_{\Delta s} \cdots \Phi_{\Delta s}^{N-\mu_s-\mu_{f1}} \Gamma_{\Delta s}] \quad (33)$$

$$\Gamma_{s3} = [\Phi_{\Delta s}^{N-\mu_s-\mu_{f1}-1} \Gamma_{\Delta s} \cdots \Gamma_{\Delta s}] \quad (34)$$

$$\Gamma_{f11} = [\Phi_{\Delta f1}^{N-1} \Gamma_{\Delta f1} \cdots \Phi_{\Delta f1}^{N-\mu_s} \Gamma_{\Delta f1}] \quad (35)$$

$$\Gamma_{f12} = [\Phi_{\Delta f1}^{N-\mu_s-1} \Gamma_{\Delta f1} \cdots \Phi_{\Delta f1}^{N-\mu_s-\mu_{f1}} \Gamma_{\Delta f1}] \quad (36)$$

$$\Gamma_{f13} = [\Phi_{\Delta f1}^{N-\mu_s-\mu_{f1}-1} \Gamma_{\Delta f1} \cdots \Gamma_{\Delta f1}] \quad (37)$$

$$\Gamma_{f21} = [\Phi_{\Delta f2}^{N-1} \Gamma_{\Delta f2} \cdots \Phi_{\Delta f2}^{N-\mu_s} \Gamma_{\Delta f2}] \quad (38)$$

$$\Gamma_{f22} = [\Phi_{\Delta f2}^{N-\mu_s-1} \Gamma_{\Delta f2} \cdots \Phi_{\Delta f2}^{N-\mu_s-\mu_{f1}} \Gamma_{\Delta f2}] \quad (39)$$

$$\Gamma_{f23} = [\Phi_{\Delta f2}^{N-\mu_s-\mu_{f1}-1} \Gamma_{\Delta f2} \cdots \Gamma_{\Delta f2}] \quad (40)$$

in which μ_s , μ_{f1} and μ_{f2} are the controllability indices of respectively slow, fast 1 and fast 2 subsystems. Let us assume K in (23) as

$$K = [K_s^T \ K_{f1}^T \ K_{f2}^T]^T \quad (41)$$

where submatrices K_s , K_{f1} and K_{f2} are respectively of dimensions $(N - \mu_{f2} - \mu_{f1})m \times p$, $\mu_{f1}m \times p$ and $\mu_{f2}m \times p$. Then using (23), (30), (31) and (41), expressions for K_s , K_{f1} and K_{f2} can be obtained as

$$K_s = [(\Gamma_{s1} - \Gamma_{s3} \Gamma_{f23}^{-1} \Gamma_{f21}) - (\Gamma_{s2} - \Gamma_{s3} \Gamma_{f23}^{-1} \Gamma_{f22}) \\ (\Gamma_{f12} - \Gamma_{f13} \Gamma_{f23}^{-1} \Gamma_{f22})^{-1} (\Gamma_{f11} - \Gamma_{f13} \Gamma_{f23}^{-1} \Gamma_{f21})]^{-1} \\ [(G_1^T - \Gamma_{s3} \Gamma_{f23}^{-1} G_3^T) - (\Gamma_{s2} - \Gamma_{s3} \Gamma_{f23}^{-1} \Gamma_{f22}) \\ (\Gamma_{f12} - \Gamma_{f13} \Gamma_{f23}^{-1} \Gamma_{f22})^{-1} (G_2^T - \Gamma_{f13} \Gamma_{f23}^{-1} G_3^T)] \quad (42)$$

$$K_{f1} = (\Gamma_{f12} - \Gamma_{f13} \Gamma_{f23}^{-1} \Gamma_{f22})^{-1} [(G_2^T - \Gamma_{f13} \Gamma_{f23}^{-1} G_3^T) \\ - (\Gamma_{f11} - \Gamma_{f13} \Gamma_{f23}^{-1} \Gamma_{f21}) K_s] \quad (43)$$

$$K_{f2} = \Gamma_{f23}^{-1} (G_3^T - \Gamma_{f21} K_s - \Gamma_{f22} K_{f1}). \quad (44)$$

Since, G stabilizes $(\Phi_\tau + GM)$ and K is an exact solution of (23), closed loop system (21) will also be stable.

Proposition 1: If fast 1 and fast 2 subsystems are assumed to be stable and an output injection gain $G^T = [G_s^T \ 0 \ 0]$ is applied to (26), then closed loop system $(\Phi_\tau + GM)$ is stable.

Proof: Since, systems (26) and (24) are related through linear transformation (28), they have the same eigenvalues. Now, if $G^T = [G_s^T \ 0 \ 0]$ is an output injection gain for (26), then closed loop system becomes

$$z_{d_{k+1}} = \begin{bmatrix} \Phi_{\tau s} + G_s M_s & 0 & 0 \\ G_s M_{f1} & \Phi_{\tau f1} & 0 \\ G_s M_{f2} & 0 & \Phi_{\tau f2} \end{bmatrix} z_{d_k}. \quad (45)$$

From above system it is clear that, $(\Phi_{\tau s} + G_s M_s)$ is stable by design and both $\Phi_{\tau f1}$ and $\Phi_{\tau f2}$ are assumed to be stable. Therefore, system (45) is stable. Using (28), system (45) can be transformed into original states, which is also stable. System (24) is three-time-scale representation of system (13). Hence, closed loop system $(\Phi_\tau + GM)$ is stable. ■

Proposition 1 suggests that for systems having stable fast 1 and fast 2 modes one might choose $G_{f1} = G_{f2} = 0$ and therefore $G_1 = G_s$ which yields reduced three-time-scale approximation to K as $\hat{K} = [\hat{K}_s^T \ \hat{K}_{f1}^T \ \hat{K}_{f2}^T]^T$, where submatrices are approximated as

$$\hat{K}_s = [(\Gamma_{s1} - \Gamma_{s3} \Gamma_{f23}^{-1} \Gamma_{f21}) - (\Gamma_{s2} - \Gamma_{s3} \Gamma_{f23}^{-1} \Gamma_{f22}) \\ (\Gamma_{f12} - \Gamma_{f13} \Gamma_{f23}^{-1} \Gamma_{f22})^{-1} (\Gamma_{f11} - \Gamma_{f13} \Gamma_{f23}^{-1} \Gamma_{f21})]^{-1} G_s^T \quad (46)$$

$$\hat{K}_{f1} = -(\Gamma_{f12} - \Gamma_{f13} \Gamma_{f23}^{-1} \Gamma_{f22})^{-1} \\ (\Gamma_{f11} - \Gamma_{f13} \Gamma_{f23}^{-1} \Gamma_{f21}) K_s \quad (47)$$

$$\hat{K}_{f2} = \Gamma_{f23}^{-1} (-\Gamma_{f21} K_s - \Gamma_{f22} K_{f1}). \quad (48)$$

Remark 1: Eigenvalues of $\Phi_{\Delta f2}$ are very small for sampling period Δ . Hence, $\Phi_{\Delta f2}$, $\Phi_{\Delta f2}^2 \cdots$ would be very small. Thus Γ_{f21} and Γ_{f22} can be neglected in comparison to Γ_{f23} in (37) to (39), which again give approximation to \hat{K} as $\bar{K} = [\bar{K}_s^T \ \bar{K}_{f1}^T \ \bar{K}_{f2}^T]^T$ where $\bar{K}_s = (\Gamma_{s1} - \Gamma_{s2} \Gamma_{f12}^{-1} \Gamma_{f11})^{-1} G_s^T$, $\bar{K}_{f1} = -\Gamma_{f12}^{-1} \Gamma_{f11} K_s$ and $\bar{K}_{f2} = 0$.

Remark II: Further, if Γ_{f1_1} is neglected in comparison to Γ_{f1_2} and Γ_{f1_3} , approximation to $\tilde{\mathbf{K}}$ as $\tilde{\mathbf{K}} = [\tilde{\mathbf{K}}_s^T \tilde{\mathbf{K}}_{f1}^T \tilde{\mathbf{K}}_{f2}^T]^T$ is obtained, where $\tilde{\mathbf{K}}_s = \Gamma_{s1}^{-1} G_s^T$ and $\tilde{\mathbf{K}}_{f1} = \tilde{\mathbf{K}}_{f2} = 0$.

IV. APPLICATION TO AHWR

A. Controller Design

The linear model of the AHWR given by (9)–(10) is found to be controllable and observable [21]. The control input, u , to RR drives consist of two terms, written as

$$u = u_g + u_s \quad (49)$$

where u_g is global power component, designed in [21], and u_s is spatial power component. Thus, system (9) becomes

$$\dot{z} = \hat{A}z + Bu_s + B_f \delta q_f \quad (50)$$

where \hat{A} , the closed loop system matrix with global power feedback as given in [21], has eigenvalues falling in three distinct clusters; first cluster of 38 eigenvalues ranging from 6.2899×10^{-3} to $(8.8268 \pm j1.8656) \times 10^{-5}$, second cluster of 35 eigenvalues that ranges from -1.8396×10^{-1} to -1.1779×10^{-2} and the third one of 17 eigenvalues ranging from -2.7626×10^2 to -7.2513 . For suitably selected sampling time, if the continuous-time system possesses three-time-scale property, its discrete version would also possess three-time-scale property [12]. In case of AHWR, choice of the sampling time is limited by the time constant characterizing the dynamics of delayed neutron precursors. The largest unstable eigenvalue of the continuous-time system (50) is 6.2899×10^{-3} , which indicate that the sampling time, $\tau < (1)/(6.2899 \times 10^{-3})$ or 159 s can be chosen. Since, the reactor power can undergo large variations in small time, it is desirable to have small sampling time from practical implementation point of view and also at the same time system should possess three-time-scale property from design point of view. Hence, τ is selected as 12 s and system (50) is discretized to obtain

$$z_{k+1} = \Phi z_k + \Gamma u_k + \Gamma_f \delta q_{fk} \quad (51)$$

$$y_k = M z_k \quad (52)$$

where $\Phi = e^{\hat{A}\tau}$, $\Gamma = \int_0^\tau e^{\hat{A}s} B ds$ and $\Gamma_f = \int_0^\tau e^{\hat{A}s} B_f ds$.

Now, the discrete-time model (51) is block-diagonalized into a slow subsystem of order 38, fast 1 subsystem of order 35 and fast 2 subsystem of order 17, with the state vector (8), partitioned as

$$z_1 = [z_H^T \quad z_X^T \quad z_f^T]^T, z_2 = [\delta h_d \quad z_C^T \quad z_x^T]^T, \quad (53)$$

$$z_3 = z_P.$$

The matrices Φ , Γ and M are partitioned accordingly. The eigenvalues of the slow, fast 1 and fast 2 subsystems agree very well respectively with the largest 38, intermediate 35 and the smallest 17 eigenvalues of the original system for sampling rate $1/\tau$. It is verified that the slow, fast 1 and fast 2 subsystems are controllable and observable. Also, it is observed that the fast 1 and fast 2 subsystems are stable. Hence, output injection matrix is designed only for the slow subsystem, so as to place

TABLE I
CLOSED LOOP EIGENVALUES

Sr. No.	Eigenvalues	Sr. No.	Eigenvalues
Slow Subsystem		Fast 1 Subsystem	
1	9.999×10^{-1}	39	8.707×10^{-1}
2	9.998×10^{-1}	40	8.249×10^{-1}
3	9.993×10^{-1}	41	5.426×10^{-1}
4	9.992×10^{-1}	42	5.412×10^{-1}
5	9.990×10^{-1}	43	5.002×10^{-1}
6	9.989×10^{-1}	44	4.992×10^{-1}
7	9.986×10^{-1}	45	4.885×10^{-1}
8	9.985×10^{-1}	46	4.884×10^{-1}
9	9.985×10^{-1}	47	4.847×10^{-1}
10	9.984×10^{-1}	48	4.830×10^{-1}
11	9.983×10^{-1}	49	4.761×10^{-1}
12	9.982×10^{-1}	50	4.755×10^{-1}
13	9.974×10^{-1}	51	4.741×10^{-1}
14	9.972×10^{-1}	52	4.730×10^{-1}
15	9.972×10^{-1}	53	4.726×10^{-1}
16	9.971×10^{-1}	54	4.718×10^{-1}
17	9.969×10^{-1}	55	4.703×10^{-1}
18	9.968×10^{-1}	56	4.701×10^{-1}
19	9.967×10^{-1}	57	2.452×10^{-1}
20	9.962×10^{-1}	58	1.711×10^{-1}
21	9.957×10^{-1}	59	1.711×10^{-1}
22	9.952×10^{-1}	60	1.691×10^{-1}
23	9.949×10^{-1}	61	1.683×10^{-1}
24	9.948×10^{-1}	62	1.542×10^{-1}
25	9.944×10^{-1}	63	1.541×10^{-1}
26	9.941×10^{-1}	64	1.527×10^{-1}
27	9.940×10^{-1}	65	1.509×10^{-1}
28	9.938×10^{-1}	66	1.411×10^{-1}
29	9.933×10^{-1}	67	1.410×10^{-1}
30	9.932×10^{-1}	68	1.396×10^{-1}
31	9.929×10^{-1}	69	1.368×10^{-1}
32	9.928×10^{-1}	70	1.148×10^{-1}
33	9.924×10^{-1}	71	1.146×10^{-1}
34	9.921×10^{-1}	72	1.137×10^{-1}
35	9.920×10^{-1}	73	1.100×10^{-1}
36	9.918×10^{-1}	Fast 2 Subsystem	
37	9.912×10^{-1}	74–90	0
38	9.907×10^{-1}		

its eigenvalues in the range of 9.9012×10^{-1} to 9.9992×10^{-1} . Finally composite output injection matrix is obtained using the method discussed in Appendix. Controllability indices of slow, fast 1 and fast 2 subsystems are found to be $\mu_s = 3$, $\mu_{f1} = 2$ and $\mu_{f2} = 1$ respectively. It can be verified that the controllability index of full order system is 6. This prompted the selection of $N = 6$. Thus, $\Delta = 2$ s. System (50) is discretized with sampling interval of Δ and block-diagonalized to formulate Γ given by (31). Here, as per Remark I, Γ_{f2_1} and Γ_{f2_3} are neglected in comparison to Γ_{f2_2} and approximated POF gain, $\tilde{\mathbf{K}}$ is obtained. The closed loop eigenvalues of the system, with this gain are given in Table I, and found to be within unit circle in z-plane.

We also tried to apply the two-time-scale POF design method by considering regrouping of states into a two-time-scale slow subsystem and fast subsystem groups as

$$w_A = [z_1] \quad (54)$$

$$w_B = [z_2 \quad z_3]. \quad (55)$$

Note that the states of the fast subsystem group are obtained by combining the fast 1 and fast 2 subsystem states of three-

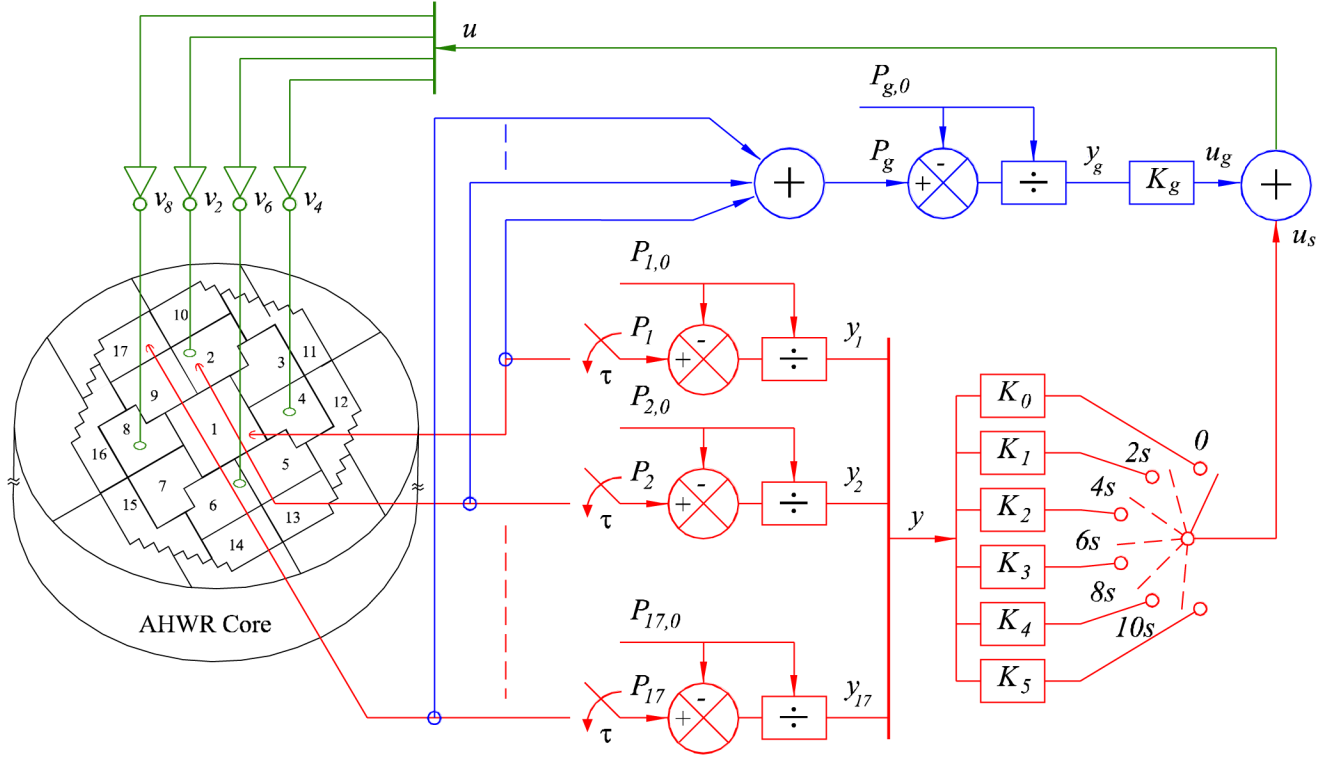


Fig. 2. Periodic output feedback based spatial controller for AHWR.

time-scale system, given by (53). However, this scheme does not work as the different matrices are as ill-conditioned as the matrices of the original system. We again tried the two-time-scale approach with following regrouping of states

$$w_1 = [z_1 \quad z_2] \quad (56)$$

$$w_2 = [z_3]. \quad (57)$$

In this formulation, the two-time-scale slow subsystem is obtained by combining the slow and fast 1 subsystems of the three-time-scale formulation. With this type of regrouping the reduction in the computation effort is not significant. Nevertheless, the ill-conditioning could successfully be obviated and the two-time-scale design method [12] could be used to obtain POF gains. In Section IV-C, the transient simulation results obtained with three-time-scale based POF design approach are compared with those of the two-time-scale POF approach and the two-time-scale FOS design approach with the state grouping given by (56) and (57).

B. Controller Implementation

Fig. 2 shows the scheme of implementation of POF based spatial controller for AHWR. The power levels of the 17 nodes in the AHWR, sensed by suitable in-core detector, are sampled periodically at the rate $1/\tau$, compared with their respective steady state values and then normalized deviations from the respective steady state levels are obtained. These are stacked as the output vector y . Subsequently $K_0 y, K_1 y, \dots, K_5 y$ are generated and the spatial component of input u_s is obtained by selecting the appropriate $K_l y (l = 0, 1, \dots, 5)$. Deviation of bulk power from

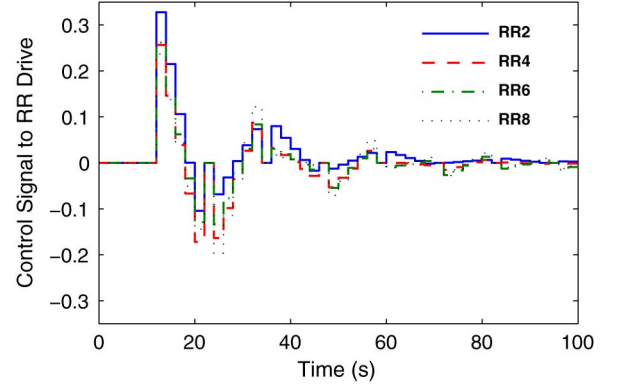


Fig. 3. Control signal to RR drives.

its steady state value is also computed and bulk power dependent term u_g is computed on a continuous basis. Then by adding u_g and u_s , so generated, the control signals v_2, v_4, v_6 and v_8 are obtained and they are applied to respective RR drives. This POF based control scheme is very similar in structure to simple output feedback based scheme, with the only difference that input is switched to different values at the input sampling instants $l = 0, 1, \dots, 5$. This is known to cause fluctuations and has been discussed at length in [9], [14]. However, as will be evident from simulation results, such fluctuations are not of any concern in this application.

C. Transient Simulations

The transient response of the closed loop system can be evaluated by simulation of vectorized nonlinear model of AHWR

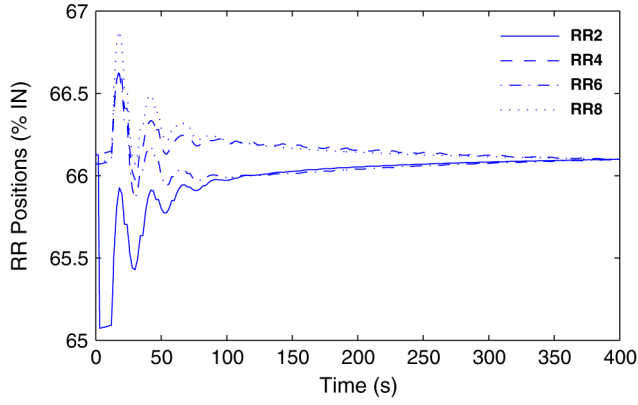


Fig. 4. Variation in RR positions.

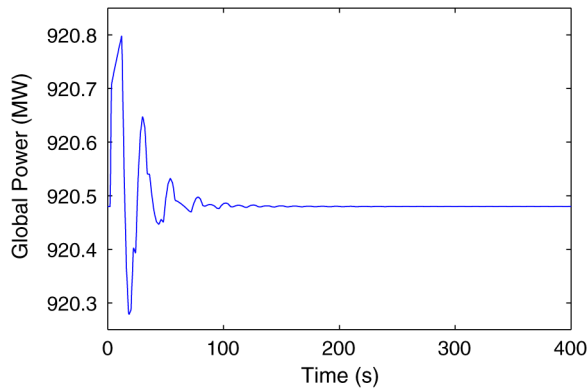


Fig. 5. Global power variations following perturbation in RR2 control signal.

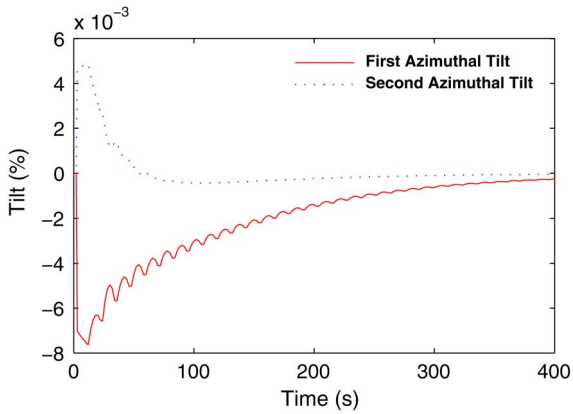
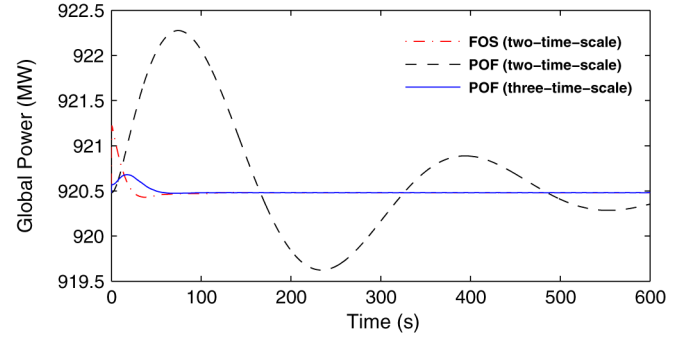
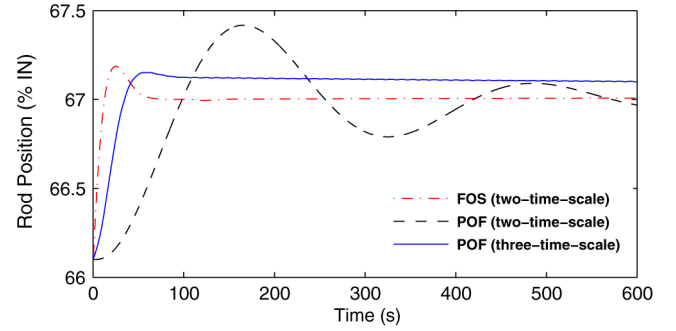


Fig. 6. Suppression of azimuthal tilts.

[22], developed from equations (1)–(7). The global power controller given by u_g was applied on continuous basis i.e. on finer time steps for controlling fast transients in the total power. To suppress spatial instabilities, computed nodal powers were sampled every $\tau = 12$ s and periodic output feedback gains K_l were applied periodically after every $\Delta = 2$ s to generate control signal $u(k\tau)$ and applied to the RR drives alongwith the signal generated by the total power controller, as discussed in Section IV-B.



(a)



(b)

Fig. 7. Variation in global power and RR positions due to positive step change of 5% in feed flow (a) Global power (MW) (b) RR positions (% IN).

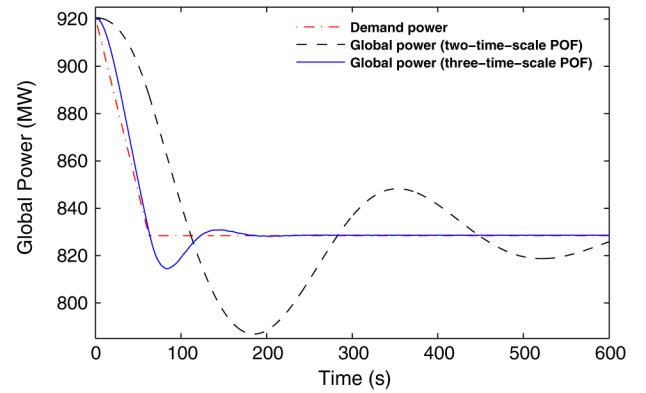


Fig. 8. Variation of global power during power maneuvering from 920.48 MW to 828.43 MW.

First consider the transient involving a spatial power disturbance. The system was initially assumed to be at full power steady state condition, with all RRs at their equilibrium positions. Shortly, RR2, originally under auto control was driven out by almost 1% manually, by giving proper control signal and left under the effect of automatic control thereafter. Fig. 3 depicts the control signals generated by the spatial power controller, and Fig. 4 depicts the corresponding RR positions. It is observed that, the total power undergoes variations between 920.8 MW and 920.2 MW and settles down at its initial value of 920.48 MW in about next 120 s, as illustrated in Fig. 5. Variations in the spatial power measured in terms of first and second azimuthal tilts [21], are suppressed within 400 s as shown in Fig. 6. No tilts were observed during a long term simulation.

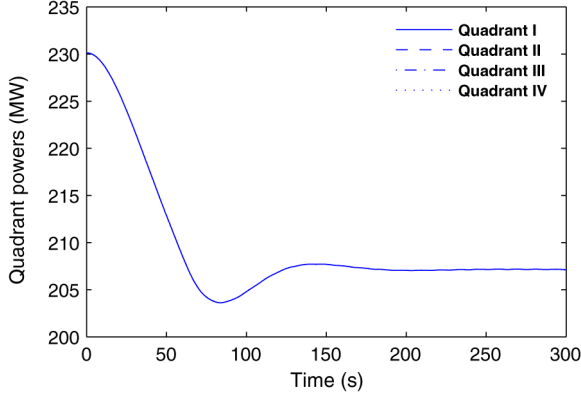


Fig. 9. Variation of quadrant powers during power maneuvering.

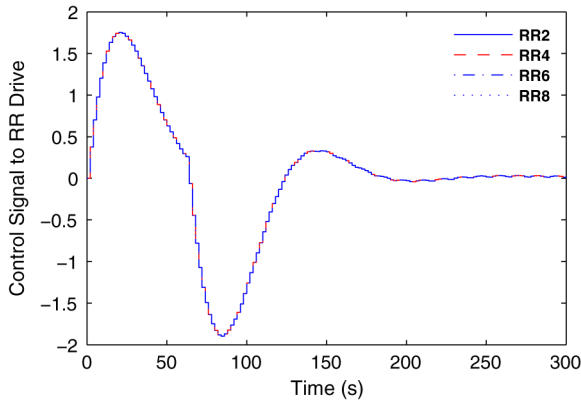


Fig. 10. Control signal to RR drives during power maneuvering from 920.48 MW to 828.43 MW.

In order to assess the response of the system to disturbances in feed flow, a scenario was simulated in which the reactor was operating at steady full power when a 5% positive step change was introduced in the feed flow. In this case, the performance of proposed controller is compared with the FOS technique [24] and periodic output feedback control, both based on the two-time-scale decomposition with the state grouping given by (56) and (57). The incoming coolant enthalpy reduced by about 0.64% and total power underwent variations as given in Fig. 7(a), from which it is also observed that, with all the control techniques the global power is stabilized after the introduction of disturbance. However, stabilization time is different. Global power stabilizes within next 100 s in FOS (two-time-scale) and POF (three-time-scale), whereas in case of POF (two-time-scale) it reaches steady state after 650 s. The overshoot is also found to be more in POF (two-time-scale) based controller than the proposed one. For compensating this step change in the feed flow, RRs are driven in by 1.02%, 0.95% and 1% respectively in POF (three-time-scale), FOS and POF (two-time-scale), as shown in Fig. 7(b). Here also, the settling time of RR positions is considerably more in case of POF (two-time-scale) approach than the other two control methods.

In another transient, initially, the reactor is under steady state and is assumed to be operating at 920.48 MW with nodal power distribution as given in [21]. Now, the demand is reduced uniformly at the rate of 1.5 MW/s to 828.43 MW, in 60 s and

held constant thereafter. During the transient, it is observed that, the global power is following the demand power as shown in Fig. 8. Again the results are compared with POF (two-time-scale), and it is found that the performance of suggested POF control is better than POF (two-time-scale) control. Fig. 9 shows the variation in quadrant powers and Fig. 10 illustrates the control signal generated by suggested POF controller. It is noted that, the xenon concentrations stabilizes to their respective new steady state values in about 40 h. However, the nodal powers attain the steady state value in 100 s.

V. CONCLUSION

In this paper, method is proposed to design periodic output feedback controller for system with slow, fast and very fast modes. This method is used for spatial stabilization of AHWR. Numerically ill-conditioned system of AHWR is first decoupled into three subsystems of lower order, namely, slow, fast 1 and fast 2 subsystems by three-stage linear transformation. POF gains for the original system are obtained by combining the solutions of the subsystem problems solved independently. Since, fast 1 and fast 2 subsystems are stable, output injection gains for these subsystems are taken as zero. Periodic output feedback gain obtained from the slow subsystem alone is applied to the AHWR and dynamic simulations are carried out under different transient conditions. As the controller is based on the feedback of outputs only, there is no need of state observer. Further the controller is compared with FOS based control technique and performance is observed to be better. Collectively, the controller performance seems satisfactory.

APPENDIX

DESIGN OF OUTPUT INJECTION GAIN

Design of output injection gain for system (26)–(27) is equivalent to design of a state feedback for its adjoint system, which is given by

$$\begin{bmatrix} \hat{z}_{s_{k+1}} \\ \hat{z}_{f1_{k+1}} \\ \hat{z}_{f2_{k+1}} \end{bmatrix} = \begin{bmatrix} \Phi_{\tau s}^T & 0 & 0 \\ 0 & \Phi_{\tau f1}^T & 0 \\ 0 & 0 & \Phi_{\tau f2}^T \end{bmatrix} \begin{bmatrix} \hat{z}_{s_k} \\ \hat{z}_{f1_k} \\ \hat{z}_{f2_k} \end{bmatrix} + \begin{bmatrix} M_s^T \\ M_{f1}^T \\ M_{f2}^T \end{bmatrix} u_k \quad (58)$$

$$y_k = [\Gamma_{\tau s}^T \quad \Gamma_{\tau f1}^T \quad \Gamma_{\tau f2}^T] [\hat{z}_{s_k}^T \quad \hat{z}_{f1_k}^T \quad \hat{z}_{f2_k}^T]^T. \quad (59)$$

If original system is controllable and observable, its adjoint system is observable and controllable [27]. Now in order to design a state feedback based controller for (58) consider three-stage pole placement problem with input u_k as $u_k = u_{s_k} + u_{f1_k} + u_{f2_k}$. In the first stage, $p \times n_1$ matrix G_s^T is designed to place eigenvalues of $(\Phi_{\tau s}^T + M_s^T G_s^T)$ at desired locations. The input u_{s_k} is computed as

$$u_{s_k} = [G_s^T \quad 0 \quad 0] \hat{z}_{d_k} \quad (60)$$

where $\hat{z}_{d_k} = [\hat{z}_{s_k}^T \hat{z}_{f1_k}^T \hat{z}_{f2_k}^T]^T$. Substituting the value of u_{s_k} from (60) into (58) yields

$$\hat{z}_{d_{k+1}} = \begin{bmatrix} \Phi_{\tau s}^T + M_s^T G_s^T & 0 & 0 \\ M_{f1}^T G_s^T & \Phi_{\tau f1}^T & 0 \\ M_{f2}^T G_s^T & 0 & \Phi_{\tau f2}^T \end{bmatrix} \hat{z}_{d_k} + \begin{bmatrix} M_s^T \\ M_{f1}^T \\ M_{f2}^T \end{bmatrix} u_{d1_k} \quad (61)$$

where $u_{d1_k} = u_{f1_k} + u_{f2_k}$. Now, for decoupling fast 1 subsystem, let us take $\hat{z}_{d1_k} = [\hat{z}_{s_k}^T \hat{z}_{f1_k}^T \hat{z}_{f2_k}^T]^T = T_{d1} \hat{z}_{d_k}$, where transformation matrix $T_{d1} \in \mathbb{R}^{n \times n}$ is given by

$$T_{d1} = \begin{bmatrix} E_{n_1} & 0 & 0 \\ N_{21} & E_{n_2} & 0 \\ N_{31} & 0 & E_{n_3} \end{bmatrix} \quad (62)$$

and $n_2 \times n_1$ matrix N_{21} and $n_3 \times n_1$ matrix N_{31} respectively satisfy $N_{21}(\Phi_{\tau s}^T + M_s^T G_s^T) + M_{f1}^T G_{f1}^T - \Phi_{\tau f1}^T N_{21} = 0$, $N_{31}(\Phi_{\tau s}^T + M_s^T G_s^T) + M_{f2}^T G_{f2}^T - \Phi_{\tau f2}^T N_{31} = 0$.

Then equivalent system is obtained as follows

$$\begin{aligned} \hat{z}_{d1_{k+1}} &= \begin{bmatrix} \Phi_{\tau s}^T + M_s^T G_s^T & 0 & 0 \\ 0 & \Phi_{\tau f1}^T & 0 \\ 0 & 0 & \Phi_{\tau f2}^T \end{bmatrix} \hat{z}_{d1_k} \\ &+ \begin{bmatrix} M_s^T \\ \bar{M}_{f1}^T \\ \bar{M}_{f2}^T \end{bmatrix} u_{d1_k} \end{aligned} \quad (63)$$

where $\bar{M}_{f1}^T = N_{21} M_s^T + M_{f1}^T$ and $\bar{M}_{f2}^T = N_{31} M_s^T + M_{f2}^T$. Systems (63) and (61) are related through linear transformation (62). As a result, when pair $(\Phi_{\tau f1}^T, M_{f1}^T)$ is controllable, pair $(\Phi_{\tau f1}^T, \bar{M}_{f1}^T)$ is also controllable. Therefore, in second stage, $p \times n_2$ matrix G_{f1}^T is designed to place eigenvalues of $(\Phi_{\tau f1}^T + \bar{M}_{f1}^T G_{f1}^T)$ at desired locations, for that input u_{f1_k} is computed as

$$u_{f1_k} = [0 \quad G_{f1}^T \quad 0] \hat{z}_{d1_k}. \quad (64)$$

Substituting this value of u_{f1_k} into (63) gives

$$\begin{aligned} \hat{z}_{d1_{k+1}} &= \begin{bmatrix} \Phi_{\tau s}^T + M_s^T G_s^T & M_s^T G_{f1}^T & 0 \\ 0 & \Phi_{\tau f1}^T + \bar{M}_{f1}^T G_{f1}^T & 0 \\ 0 & \bar{M}_{f2}^T G_{f1}^T & \Phi_{\tau f2}^T \end{bmatrix} \hat{z}_{d1_k} \\ &+ \begin{bmatrix} M_s^T \\ \bar{M}_{f1}^T \\ \bar{M}_{f2}^T \end{bmatrix} u_{f2_k}. \end{aligned} \quad (65)$$

Now, fast 2 subsystem is decoupled using $\hat{z}_{d2_k} = [\hat{z}_{s_k}^T \hat{z}_{f1_k}^T \hat{z}_{f2_k}^T]^T = T_{d2} \hat{z}_{d1_k}$, where transformation matrix $T_{d2} \in \mathbb{R}^{n \times n}$ is given by

$$T_{d2} = \begin{bmatrix} E_{n_1} & N_{12} & 0 \\ 0 & E_{n_2} & 0 \\ 0 & N_{32} & E_{n_3} \end{bmatrix} \quad (66)$$

and $n_1 \times n_2$ matrix N_{12} and $n_3 \times n_2$ matrix N_{32} satisfy $M_s^T G_{f1}^T + N_{12}(\Phi_{\tau f1}^T + \bar{M}_{f1}^T G_{f1}^T) - (\Phi_{\tau s}^T + M_s^T G_s^T) N_{12} = 0$, $\bar{M}_{f2}^T G_{f1}^T + N_{32}(\Phi_{\tau f1}^T + \bar{M}_{f1}^T G_{f1}^T) - \Phi_{\tau f2}^T N_{32} = 0$.

Then we obtain the following equivalent system

$$\begin{aligned} \hat{z}_{d2_{k+1}} &= \begin{bmatrix} \Phi_{\tau s}^T + M_s^T G_s^T & 0 & 0 \\ 0 & \Phi_{\tau f1}^T + \bar{M}_{f1}^T G_{f1}^T & 0 \\ 0 & 0 & \Phi_{\tau f2}^T \end{bmatrix} \hat{z}_{d2_k} \\ &+ \begin{bmatrix} \bar{M}_s^T \\ \bar{M}_{f1}^T \\ \bar{M}_{f2}^T \end{bmatrix} u_{f2_k} \end{aligned} \quad (67)$$

where $\bar{M}_s^T = M_s^T + N_{12} \bar{M}_{f1}^T$ and $\bar{M}_{f2}^T = N_{32} \bar{M}_{f1}^T + \bar{M}_{f2}^T$. Finally let input u_{f2_k} is computed as

$$u_{f2_k} = [0 \ 0 \ G_{f2}^T] \hat{z}_{d2_k}. \quad (68)$$

where G_{f2}^T is designed to place eigenvalues of $(\Phi_{\tau f2}^T + \bar{M}_{f2}^T G_{f2}^T)$ at desired locations. Now from (60), (64) and (68), the composite control $u_k = u_{s_k} + u_{f1_k} + u_{f2_k}$ is given by

$$\begin{aligned} u_k &= [G_s^T \ 0 \ 0] \hat{z}_{d_k} + [0 \ G_{f1}^T \ 0] \hat{z}_{d1_k} + [0 \ 0 \ G_{f2}^T] \hat{z}_{d2_k} \\ &= ([G_s^T \ 0 \ 0] + [0 \ G_{f1}^T \ 0] T_{d1} + [0 \ 0 \ G_{f2}^T] T_{d2} T_{d1}) \hat{z}_{d_k} \end{aligned}$$

which turns out to be

$$u_k = [G_1^T \quad G_2^T \quad G_3^T] \hat{z}_{d_k} \quad (69)$$

$$= [G_1^T \quad G_2^T \quad G_3^T] T \hat{z}_k \quad (70)$$

where

$$\begin{aligned} G_1^T &= G_s^T + G_{f1}^T N_{21} + G_{f2}^T N_{32} N_{21} + G_{f2}^T N_{31}, \\ G_2^T &= G_{f1}^T + G_{f2}^T N_{32}, \\ G_3^T &= G_{f2}^T. \end{aligned}$$

where \hat{z}_k is the state vector of adjoint system of (24).

ACKNOWLEDGMENT

The authors would like to express their sincere thanks to the Board of Research in Nuclear Sciences (BRNS), Department of Atomic Energy, Government of India for funding the project (Sanction No. 2009/36/102-BRNS). The authors would also like to express their sincere thanks to Shri. C. K. Pithawa (Director, E&IG) and Shri. Y. S. Mayya (Head, Reactor Control Division (RCnD)) of Bhabha Atomic Research Centre (BARC) for their guidance and encouragement. Thanks are also due to Shri. Ranjit Kumar, RCnD, BARC for his effort in preparing the figures included in this paper.

REFERENCES

- [1] P. V. Kokotovic, R. E. O'Malley, and P. Sannuti, "Singular perturbations and order reduction in control theory-an overview," *Automatica*, vol. 12, pp. 123–132, Mar. 1976.
- [2] V. R. Saksena, J. O'Reilly, and P. V. Kokotovic, "Singular perturbations and time-scale methods in control theory: Survey 1976-1983," *Automatica*, vol. 20, pp. 273–293, May 1984.
- [3] S. R. Shimjith, A. P. Tiwari, and B. Bandyopadhyay, "A three-time-scale approach for design of linear state regulator for spatial control of advanced heavy water reactor," *IEEE Trans. Nucl. Sci.*, vol. 58, no. 3, pt. 3, pp. 1264–1276, Jun. 2011.
- [4] R. G. Phillips, "A two-stage design of linear feedback controls," *IEEE Trans. Autom. Control*, vol. 25, no. 6, pp. 1220–1223, Dec. 1980.
- [5] D. S. Naidu, *Singular Perturbation Methodology in Control Systems*. London, U.K.: Peter Peregrinus Ltd., 1988.
- [6] R. G. Phillips, "Reduced order modeling and control of two-time-scale discrete systems," *Int. J. Control*, vol. 31, no. 4, pp. 765–780, 1980.
- [7] V. L. Syrmos, C. T. Abdallah, P. Dorato, and K. Grigoriadis, "Static output feedback-a survey," *Automatica*, vol. 33, pp. 125–137, Feb. 1997.
- [8] A. B. Chammas and C. T. Leondes, "Pole assignment by piecewise constant output feedback," *Inter. J. Control*, vol. 29, pp. 31–38, 1979.
- [9] H. Werner and K. Furuta, "Simultaneous stabilization based on output measurement," *Kybernetika*, vol. 31, pp. 395–414, 1995.

- [10] B. M. Patre and B. Bandyopadhyay, "Periodic output feedback control for two-time-scale discrete systems," in *Proc. IEEE TENCON*, Dec. 1998, vol. 1, pp. 174–177.
- [11] B. M. Patre, B. Bandyopadhyay, and H. Werner, "Periodic output feedback control for singularly perturbed discrete model of steam power system," in *Proc. IEE Contr. Theory Appl.*, May 1999, vol. 146, pp. 247–252.
- [12] A. P. Tiwari, G. D. Reddy, and B. Bandyopadhyay, "Design of periodic output feedback and fast output sampling based controllers for systems with slow and fast modes," *Asian J. Control*, vol. 14, pp. 271–277, Jan. 2012.
- [13] B. M. Patre, B. Bandyopadhyay, and H. Werner, "Control of discrete two-time-scale system by using piecewise constant periodic output feedback," *Syst. Sci. J.*, vol. 23, pp. 23–38, 1997.
- [14] A. P. Tiwari, B. Bandyopadhyay, and H. Werner, "Spatial control of a large PHWR by piecewise constant periodic output feedback," *IEEE Trans. Nucl. Sci.*, vol. 47, no. 2, pt. 2, pp. 389–402, Apr. 2000.
- [15] D. B. Talange, B. Bandyopadhyay, and A. P. Tiwari, "Spatial control of a large PHWR by decentralized periodic output feedback and model reduction techniques," *IEEE Trans. Nucl. Sci.*, vol. 53, no. 4, pt. 2, pp. 2308–2317, Aug. 2006.
- [16] R. K. Sinha and A. Kakodkar, "Design and development of the AHWR-the indian thorium fuelled innovative nuclear reactor," *Nucl. Eng. Design*, vol. 236, pp. 683–700, Apr. 2006.
- [17] J. J. Duderstadt and L. J. Hamilton, *Nuclear Reactor Analysis*. Hoboken, NJ, USA: Wiley, Jan. 1976.
- [18] S. R. Shimjith, A. P. Tiwari, M. Naskar, and B. Bandyopadhyay, "Space-time kinetics modeling of advanced heavy water reactor for control studies," *Annals Nucl. Energy*, vol. 37, pp. 310–324, Mar. 2010.
- [19] S. R. Shimjith, A. P. Tiwari, and B. Bandyopadhyay, "Coupled neutronics-thermal hydraulics model of advanced heavy water reactor for control system studies," in *Proc. IEEE INDICON, IIT*, Dec. 2008, pp. 126–131.
- [20] K. J. Astrom and R. D. Bell, "Drum-boiler dynamics," *Automatica*, vol. 36, pp. 363–378, Mar. 2000.
- [21] S. R. Shimjith, A. P. Tiwari, B. Bandyopadhyay, and R. K. Patil, "Spatial stabilization of advanced heavy water reactor," *Annals Nucl. Energy*, vol. 38, pp. 1545–1558, Jul. 2011.
- [22] R. K. Munje, B. M. Patre, and A. P. Tiwari, "Non-linear simulation and control of xenon induced oscillations in advanced heavy water reactor," *Annals Nucl. Energy*, vol. 64, pp. 191–200, Feb. 2014.
- [23] S. R. Shimjith, A. P. Tiwari, and B. Bandyopadhyay, "Design of fast output sampling controller for three-time-scale systems: Application to spatial control of advanced heavy water reactor," *IEEE Trans. Nucl. Sci.*, vol. 58, no. 6, pt. 2, pp. 3305–3316, Dec. 2011.
- [24] R. K. Munje, P. S. Londhe, J. G. Parkhe, B. M. Patre, and A. P. Tiwari, "Spatial control of advanced heavy water reactor by fast output sampling technique," in *Proc. IEEE Control Appl.*, Aug. 2013, pp. 1212–1217.
- [25] P. S. Londhe, B. M. Patre, and A. P. Tiwari, "Design of single-input fuzzy logic controller for spatial control of advanced heavy water reactor," *IEEE Trans. Nucl. Sci.*, vol. 61, no. 2, pp. 901–911, Apr. 2014.
- [26] R. K. Munje, B. M. Patre, S. R. Shimjith, and A. P. Tiwari, "Sliding mode control for spatial stabilization of advanced heavy water reactor," *IEEE Trans. Nucl. Sci.*, vol. 60, no. 4, pt. 2, pp. 3040–3050, Aug. 2013.
- [27] C.-T. Chen, *Linear System Theory and Design*. New York, NY, USA: Oxford University Press, 1999.